Eckardt frame theory of interacting electrons in quantum dots

P. A. Maksym
Department of Physics and Astronomy, University of Leicester, University Road, Leicester LE1 7RH, United Kingdom
(Received 20 October 1995)

A transformation to a moving frame (the Eckardt frame) is used to study the quantum states of interacting electrons in parabolic quantum dots in the presence of a perpendicular magnetic field. The approach is motivated by examining ground-state pair-correlation functions obtained by exact diagonalization. The main results concern the physical nature of the electron states and the origin of magic numbers. Some of the states are found to be localized about a single minimum of the potential energy. They have well-defined symmetry and are physically analogous to molecules. They are treated approximately by antisymmetrizing Eckardt frame rotational-vibrational states. This approach leads to selection rules that predict all the magic angular momentum and spin combinations found in previous numerical work. In addition, it enables the ground-state energy and low-lying excitations of the molecular states to be calculated to high accuracy. Analytic results for three electrons agree very well with the results of exact diagonalization. States that are not localized about a single minimum are also studied. They do not have distinct spatial symmetry and occur only when selection rules and conservation laws allow tunneling between states localized on different minima. These states appear to be small system precursors of fractional quantum Hall liquids.

I. INTRODUCTION

Quantum dots are semiconductor nanostructures in which electrons are confined by a lateral potential applied in the plane of a two-dimensional system. For instance, a modulated gate electrode close to a quantum well[1] or heterojunction[2] can provide the potential necessary to confine very small (<10) numbers of electrons. Recent experimental work has explored phenomena such as quantum dot charging,[1] transport through dots,[3,4] and far-infrared absorption.[2] Related theoretical studies have led to interesting predictions such as the existence of magic angular momentum and spin quantum numbers for interacting electrons in dots.[5,6] These are the only possible angular momenta and spins of the ground state and if a dot is placed in a magnetic field, transitions from one magic value to another can be induced by changing the magnetic field. This is predicted to cause oscillations in physical properties such as electronic heat capacity,[5] magnetization,[6,7] and luminescence[8] and to affect transport[9,10] and optical properties[11,12] and the chemical potential.[13–15] There is evidence that some of the predicted transitions have been observed.[1,13] Another interesting theoretical prediction concerns the nature of the ground state. Under certain circumstances it is predicted to have some order whose form is determined by the equilibrium between the confinement and the Coulomb interaction.[16–20] The physical picture of these states is that of a molecule and sometimes they are described as ''Wigner molecules.'' The present work is concerned both with magic numbers and electron states. The general idea is to consider the dynamics in a moving frame of reference. This explains why the magic numbers occur, enables the ''molecular'' energy levels to be calculated accurately, and gives insight into the physical nature of the electron states.

Intuitively, it is clear that the minimum energy state of confined classical electrons is highly symmetric. For example, three classical electrons constrained to move in two dimensions and confined by a central potential would have a configuration in the form of a rotating equilateral triangle. It is less obvious that this kind of symmetry appears in quantum mechanics; nevertheless, pair-correlation functions for quantum ground states, presented in this work, do exhibit some symmetry, particularly for large angular momenta. This suggests that it would be useful to examine the quantum mechanics in a moving frame of reference chosen to remove the rotational motion and make the symmetry apparent. However, it is not possible to decouple the rotational motion completely because Coriolis forces appear in the moving frame. This problem is related to the question of finding a reference frame to describe the vibrational motion of a rotating molecule. There is no reference frame in which the vibrational motion is completely decoupled from the rotational motion but there is a frame, known as the Eckardt frame, in which the mechanical angular momentum associated with the vibrational motion vanishes to first order in displacements.[21] This reference frame is used here to study the quantum states of interacting electrons in quantum dots.

In the minimum energy state of N confined classical electrons, each electron orbits in such a way that the electron configuration as a whole rotates rigidly and has well-defined symmetry. The classical excitations are vibrations about this configuration which appear in the Eckardt frame. If the quantum ground state is localized about one of the classical minima it should have the same symmetry as the classical minimum and its excitations should be quantized vibrations. This is the reason for developing a theory in which the Eckardt frame is used and electron states are approximated by antisymmetrized rotational-vibrational states. It turns out that this approach can be very accurate. All of the known magic numbers emerge from selection rules that determine when an antisymmetric electron state can be constructed from the rotational-vibrational ground state. In addition, the

rotational-vibrational energies can provide a very good approximation to the energy of the electron ground state and its excitations (accurate up to one part in 10 000 for three electrons). There are of course quantum states which are not localized about a single classical minimum. They arise from quantum tunneling between minima of different symmetry and do not have symmetry that is characteristic of any single minimum. The tunneling is governed by selection rules and conservation laws that only allow it to occur for a subset of the possible ground-state quantum numbers. Thus the ground states may be classified into two types: those that are localized about a single minimum, where the physical picture is ''molecular,'' and those that are spread over more than one minimum, where the physical picture is ''liquidlike.'' (The term ''liquidlike'' is used here to describe the loss of symmetry that occurs when states on different minima are allowed to mix.) It turns out that the liquidlike states only occur at the same filling factors as fractional quantum Hall liquids.

In brief, the main results of this paper are the relation between the magic numbers and the symmetry of classical minima, the accuracy of the vibrational approximation for the ''molecular'' states, and the analysis of the effects of tunneling. The paper opens with a summary of the current theoretical model of quantum dots (Sec. II). This is followed by numerical results on pair-correlation functions (Sec. III) which are used to demonstrate the symmetry of the quantum ground states and make the intuitive remarks of the last two paragraphs more precise. Sections IV and V deal with classical and quantum rotational-vibrational motion and give generalizations that are needed to apply results from molecular physics to quantum dots. In particular, it is necessary to allow for the presence of a magnetic field, determine the equilibrium configuration, and deal with Coriolis coupling. (Unlike molecules, quantum dots have strong Coriolis coupling and this must be treated exactly to obtain accurate results.) The connection between the magic numbers and the symmetry of the classical equilibrium configurations is made in Sec. V. Section VI gives an analytic treatment of the vibrational approximation for three electrons which is used to illustrate the general theory and demonstrate its accuracy. The effects of tunneling are covered in Sec. VII and the paper closes with a discussion of the implications of this work (Sec. VIII). Two appendixes contain technical details. Preliminary reports of some parts of this work are available in the literature.[19,20]

II. PARABOLIC QUANTUM DOTS

The present work is concerned with electrons that are constrained to move in a plane and are confined by a parabolic potential applied within this plane. It is accepted that this model of a quantum dot contains all the essential physics although there is evidence that some details need to be improved before it can be used to match real experimental data.[24,25] The Hamiltonian is

$$H=\sum_{i=1}^{N}\left\{\frac{1}{2m^*}[\mathbf{p}_i+e\mathbf{A}(\mathbf{r}_i)]^2+\frac{1}{2}m^*\omega_0^2 r_i^2\right\}+\frac{1}{2}\left(\frac{e^2}{4\pi\epsilon\epsilon_0}\right)\sum_{i=1}^{N}\sum_{\substack{j=1\\ j\neq i}}^{N}\frac{1}{|\mathbf{r}_i-\mathbf{r}_j|}+g^*\mu_B BS_z, \quad (1)$$

where the first term is the one-electron term, the second term is the Coulomb interaction term, and the last term is the Zeeman energy. The magnetic field $B\hat{\mathbf{k}}$ is perpendicular to the plane of the dot, the confinement energy is $\hbar\omega_0$, m^* is the effective electron mass, g^* is the effective g factor, and ϵ is the dielectric constant. The circular gauge is used and the magnetic vector potential, $\mathbf{A}=(B/2)(\hat{\mathbf{k}}\times\mathbf{r})$.

Without interaction the eigenstates of the system would be antisymmetrized products of the states of the one-electron Hamiltonian. These one-electron states are the well-known Fock-Darwin states which have the form

$$\psi_{nl}(\mathbf{r})=\frac{1}{\sqrt{2\pi\lambda^2}}\left[\frac{n!}{(n+|l|)!}\right]^{\frac{1}{2}}\left(\frac{r}{\sqrt{2}\lambda}\right)^{|l|}\times L_n^{|l|}(r^2/2\lambda^2)\exp(-r^2/4\lambda^2)\exp(-il\phi), \quad (2)$$

with energies given by

$$E_{nl}=(2n+1+|l|)\hbar\Omega-l\hbar\omega_c/2, \quad (3)$$

where the $L_n^{|l|}$ are associated Laguerre polynomials, $\lambda^2=\hbar/(2m^*\Omega)$, $\Omega^2=\omega_0^2+\omega_c^2/4$, and ω_c is the cyclotron frequency, eB/m^*. The parameter λ is a measure of the length scale of the system, both in the interacting and noninteracting case, and it is sometimes convenient to use it as the length unit.

Theoretical and numerical results are compared throughout this work. In all cases results are for GaAs dots ($m^*=0.067$, $g^*=-0.44$, $\epsilon=12.4$) with a confinement energy of 4 meV. This is a little larger than typical experimental values (2–3 meV) and is deliberately chosen to allow trends to be illustrated without running numerical calculations for excessively large angular momentum values.

III. NUMERICAL CHARACTERIZATION OF ELECTRON STATES

A. Correlation functions

Quantum states of interacting electrons are often characterized by the electron density or the pair distribution function but these functions are unsuitable in the present case because they only depend on distances. This means that they are insensitive to angular correlations which turn out to be very important in quantum dots, particularly so in the limit of large angular momentum. A better way of characterizing the states is to use the pair-correlation function $P_{ss'}(\mathbf{r},\mathbf{r}_0)$, defined by the equation,

$$P_{ss'}(\mathbf{r},\mathbf{r}_0)=\frac{(2\pi\lambda^2)^2}{N(N-1)}\left\langle\sum_{i\neq j}\delta(\mathbf{r}_i-\mathbf{r})\,\delta_{ss_i}\delta(\mathbf{r}_j-\mathbf{r}_0)\,\delta_{s's_j}\right\rangle, \quad (4)$$

where the angular brackets denote the expectation value for the state to be characterized and s,s',s_i,s_j denote spins. The vector $\mathbf{r}_0$ is fixed while $\mathbf{r}$ is varied so the resulting function of $\mathbf{r}$ is proportional to the probability of finding an electron at $\mathbf{r}$ given that there is one at $\mathbf{r}_0$. Roughly speaking, use of this function enables rotational motion to be ''frozen'' which allows the angular distribution to be ''seen.'' The normalization of P is chosen such that it is normalized to unity when lengths are measured in units of λ. That is, $1/(2\pi)^2\Sigma_{s=1}^{N}\Sigma_{s'=1}^{N}\int P_{ss'}(\mathbf{r}',\mathbf{r}'_0)d\mathbf{r}'d\mathbf{r}'_0=1$, where $\mathbf{r}'$ and $\mathbf{r}'_0$ are dimensionless. This normalization is convenient for numerical calculations and is consistent with the normalization of the pair-distribution function used in previous work.[26] The electron density, $n_s(r)$, and pair-distribution functions, $g_{ss'}(r)$, can be obtained by integrating $P_{ss'}(\mathbf{r},\mathbf{r}_0)$:

$$n_s(r)=\frac{N}{(2\pi\lambda^2)^2}\sum_{s'}\int P_{ss'}(\mathbf{r},\mathbf{r}_0)d\mathbf{r}_0, \tag{5}$$

$$g_{ss'}(r)=\frac{1}{2\pi\lambda^2}\int P_{ss'}(\mathbf{r}+\mathbf{r}_0,\mathbf{r}_0)d\mathbf{r}_0. \tag{6}$$

It may be shown that the integrals only depend on r when the dot is parabolic; thus the angular information in $P_{ss'}(\mathbf{r},\mathbf{r}_0)$ is eliminated when it is integrated to obtain $n_s(r)$ and $g_{ss'}(r)$.

B. Classical equilibrium configurations

The shape of $P_{ss'}(\mathbf{r},\mathbf{r}_0)$ clearly depends on $\mathbf{r}_0$. Extensive numerical studies have shown that $P_{ss'}(\mathbf{r},\mathbf{r}_0)$ generally takes its largest values when r_0 is close to the radius of the classical minimum energy (or equilibrium) configuration. Further, $P_{ss'}(\mathbf{r},\mathbf{r}_0)$ rotates rigidly when $\mathbf{r}_0$ is rotated so the only nontrivial influence on the shape is via r_0. For up to five electrons the classical equilibrium configuration is ring shaped and rotates in such a way that the electrons remain equidistantly spaced around the ring. For six and seven electrons the minimum energy configuration is also ring shaped but there is one electron at the center of the ring. These configurations are the same as those found by Bedanov and Peeters[22] for nonrotating classical systems. In the rotating case they correspond to the Lagrangian orbits that are well known in celestial mechanics.[27] Indeed, the methods of celestial mechanics can be used to determine them, although a different approach is used in the present work (Sec. IV). Once the shape of the minimum energy configuration is known it is very easy to determine its size, as defined by the radius a of the largest orbit. The Hamiltonian, E_0, of a configuration rotating about its center of mass may be written in the form

$$E_0=\frac{L^2}{2I_0(a)}+\frac{e^2N\alpha_N}{4\pi\epsilon\epsilon_0 a}+\frac{1}{2}I_0(a)\Omega^2+\frac{\omega_c}{2}L, \tag{7}$$

where the center of mass is stationary, $L\equiv-\hbar J$ is the total angular momentum, I_0 is the equilibrium moment of inertia, and α_N is a Madelung constant which can be determined from the total electrostatic energy. For an N-fold ring with N electrons $\alpha_N=s_N\equiv\Sigma_{i=1}^{N-1}[4|\sin(\phi_i/2)|]^{-1}$, where the ϕ_i are the distinct angles subtended at the center of the ring by pairs of electrons. For an $(N-1)$-fold ring, with one electron at the center, $N\alpha_N=(N-1)(s_{N-1}+1)$. The moment of inertia has the form $I_0(a)=m^*a^2\Sigma_i a_i'^2\equiv m^*a^2I_0'$, where the a_i' are dimensionless numbers that depend on the shape of the configuration. Minimizing E_0 leads to the equation

$$\left(\frac{L}{I_0(a)}\right)^2+\frac{e^2}{4\pi\epsilon\epsilon_0}\frac{N\alpha_N}{aI_0(a)}-\Omega^2=0, \tag{8}$$

which determines a. The exact solution can be found by Newton-Raphson iteration but an approximation useful in the limit of large $|L|$ is

$$a=\sqrt{\frac{|L|}{m^*I_0'\Omega}}+O\left(\frac{1}{|L|}\right). \tag{9}$$

Physically, this means that the Coulomb interaction only has a small effect on the orbit radii when the angular momentum is large. Unless otherwise stated all the pair-correlation functions shown in the present work were calculated with $\mathbf{r}_0$ on the x axis with r_0 determined from the exact solution of Eq. (8).

C. Numerical results

The pair-correlation functions are calculated for ground states of systems with different numbers of electrons. It is well known that the ground state only has certain magic combinations of angular momentum and spin values[5–8,10,19,24] which are dependent on the number of electrons. For example, the ground state of three spin-polarized electrons always has an angular momentum quantum number that is a multiple of 3. Readers unfamiliar with this feature are urged to look ahead to Fig. 3 where numerical results for three interacting electrons are given. The figure shows the ground-state energy as a function of total angular momentum at a fixed value of the magnetic field. Small minima occur when the angular momentum is a multiple of 3. The ground-state angular momentum is always one of the magic numbers, but the value that occurs is dependent on the magnetic field and the confinement energy. With increasing magnetic field, a series of transitions occurs in which states of increasing angular momentum become the absolute ground state. Thus it is necessary to vary the magnetic field to obtain a state with a particular angular momentum. This has been done in the present work to obtain a selection of correlation functions that are typical of the high angular momentum limit.

Figure 1 shows pair-correlation functions for magic ground states of two to seven spin-polarized electrons. The electron numbers, angular momenta, and magnetic fields at which the states occur are indicated in the figure. The black spots indicate $\mathbf{r}_0$ and the length unit is 1.89 nm. The figure is meant to show the qualitative form of $P_{ss}(\mathbf{r},\mathbf{r}_0)$ and in particular its symmetry. The contours were obtained by numerically diagonalizing the Hamiltonian within the lowest Landau level. Because the magnetic field and angular momentum are so large the higher Landau levels introduce corrections of only a few percent. In addition it has been shown[19] that inclusion of the higher Landau levels does not alter the qualitative form of $P_{ss}(\mathbf{r},\mathbf{r}_0)$. It is clear that the positions of the maxima in $P_{ss}(\mathbf{r},\mathbf{r}_0)$, together with the po-

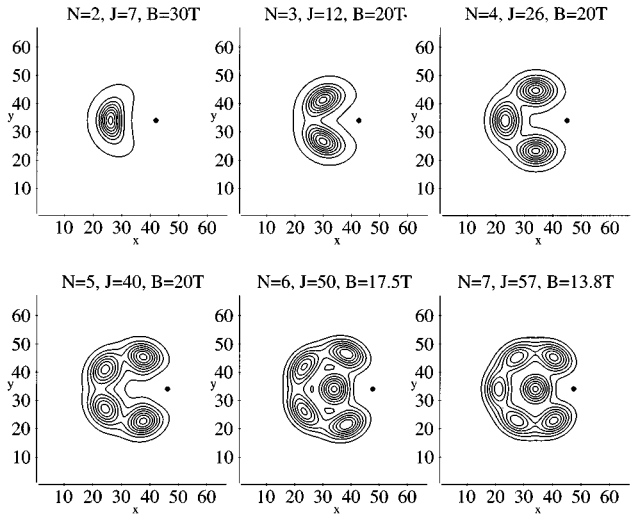

FIG. 1. Pair-correlation function $P_{ss'}(\mathbf{r},\mathbf{r}_0)$ for magic ground states of two (upper left frame) to seven (lower left frame) spin-polarized interacting electrons. The black spots denote $\mathbf{r}_0$. The x and y unit is 1.89 nm.

sition of the fixed electron, have the same symmetry as the classical minimum energy configuration. For example, for three electrons the two maxima and the fixed electron form the corners of an equilateral triangle. Ring-shaped configurations occur for up to five electrons but for six and seven electrons there is a maximum in the center of an $(N-1)$-fold ring. The maxima for six and seven electrons are not quite as sharp or symmetric as those for five or fewer electrons because the six and seven electron states were calculated for lower magnetic fields than those for five or fewer electrons. This was necessary because the calculation of $P_{ss}(\mathbf{r},\mathbf{r}_0)$ is quite expensive but it means that the angular momenta of the six and seven electron states are low relative to those for fewer electrons. This is best viewed in terms of the effective filling factor,[28] $\nu=N(N-1)/2J$. For five electrons $\nu=0.25$ while for seven electrons it is 0.37.

Figure 2 illustrates how $P_{ss}(\mathbf{r},\mathbf{r}_0)$ changes when various parameters are changed and in addition illustrates the electron density. All the frames are for three interacting spin-polarized electrons. For comparative purposes the bottom center frame shows $P_{ss}(\mathbf{r},\mathbf{r}_0)$ for the $J=12$ state shown in Fig. 1. The effect of increasing J is shown in the bottom left frame. It is clear that both the size of the triangular ring and the sharpness of the peaks increase when J is increased to 30 (which corresponds to an excited state at $B=20$ T). The top three frames are surface plots which show the effect of changing $\mathbf{r}_0$. In the top center frame r_0 is as given by Eq. (8) but in the top left frame it is decreased by 50% while in the top right frame it is increased by 50%. The actual value of r_0 is $r_0'\lambda$ where $\lambda=5.66$ nm and the value of r_0' is indicated in the figure. The main effect of changing r_0 is to change the heights of the peaks. They are clearly largest when r_0 is as given by Eq. (8). The electron density of the $J=12$ state is shown in the contour plot in the bottom right frame. Four Landau levels were used to calculate it to an accuracy of better than 1%. The density has a ring-shaped maximum whose radius is close to the classical radius given by Eq. (8). In fact, this equation gives a radius of 16.2 nm while the numerically calculated density has its maximum at a radius of 15.6 ± 0.3 nm. The uncertainty is due to the grid size used in the numerical calculation and this is also responsible for the small jitter on some of the density contours.

D. Motivation for Eckardt frame theory

The symmetry of $P_{ss}(\mathbf{r},\mathbf{r}_0)$ suggests that a good physical picture of the states characterized here is that of a rotating and vibrating molecule and the agreement of the classical

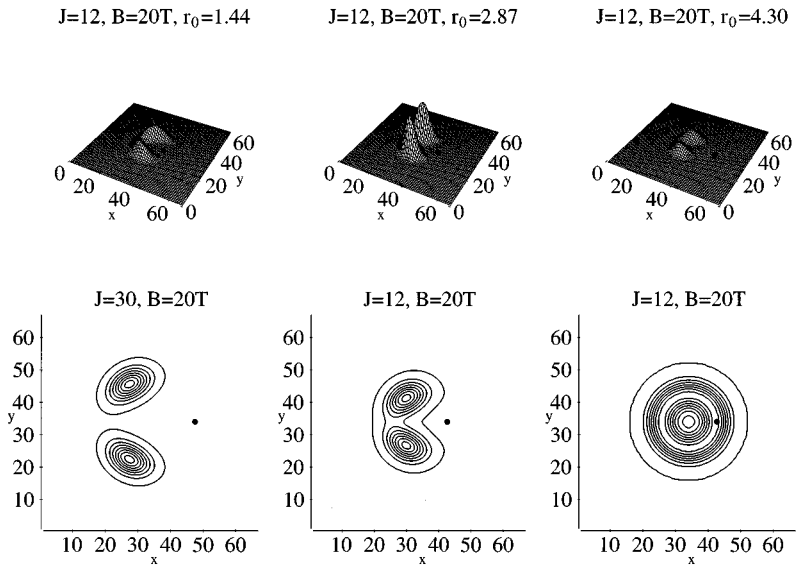

FIG. 2. Pair-correlation functions and electron density for three interacting, spin-polarized electrons. The upper frames show how the pair-correlation function, $P_{ss'}(\mathbf{r},\mathbf{r}_0)$, for $J=12$ evolves when $\mathbf{r}_0$ (black spot) is changed as described in the text. The lower left and center frames show $P_{ss'}(\mathbf{r},\mathbf{r}_0)$ for $J=30$ and $J=12$ while the lower right frame shows electron density contours for $J=12$. The x and y unit is 1.89 nm.

three-electron radius with the radius of the maximum in the three-electron density suggests that this picture should be accurate. This confirms the intuitive remarks made in the Introduction and provides the motivation for developing a theory in which the starting point is the classical equilibrium configuration and in which electron states are approximated by rotational-vibrational states that are localized about this configuration. The Eckardt frame then appears naturally as the reference frame in which the equilibrium configuration is stationary. There are actually $N!$ equilibrium configurations, each corresponding to a different permutation of the electrons. Some of these configurations are connected by permutations that are equivalent to rotations but there are other configurations which are not connected by rotations. For example, a configuration of three electrons at the corners of an equilateral triangle with vertices labeled (123) in a clockwise sense can be rotated into the configuration (312) but cannot be rotated into the configuration (213). The configurations that cannot be connected by rotations will be called *symmetrically equivalent*—a term borrowed from molecular physics.[29] A harmonic expansion can be done about any of the symmetrically equivalent configurations and the quantum vibrational states localized on each symmetrically equivalent configuration are degenerate. The electron states are then approximated by antisymmetrizing these degenerate states. The vibrational states have symmetry that is characteristic of the equilibrium configuration and it turns out that this symmetry leads to selection rules that restrict the angular momentum and spin combinations of the ground state to the known magic numbers. Thus the magic numbers are a consequence of the symmetry shown in Fig. 1. It is important to remember that the magic numbers will emerge from an approximation in which tunneling between symmetrically equivalent minima is neglected. In reality this effect breaks the degeneracy of states centered on the symmetrically equivalent minima and can affect the magic numbers. However, it turns out that the splitting of the degenerate states is very small unless the total angular momentum is small. The effects of tunneling are examined more quantitatively in Sec. VII after the vibrational approximation has been treated in detail and compared with the results of exact diagonalization. Section VII also contains a discussion of symmetrically *inequivalent* minima, that is, competing classical minima which have similar energies but different types of symmetry. In this case quantum tunneling is much more important and leads to the liquidlike states mentioned in the Introduction.

IV. CLASSICAL ROTATIONAL-VIBRATIONAL STATES

A. Classical Hamiltonian

Before stating the vibrational-rotational Hamiltonian it is necessary to be precise about the reference frame in which the vibrational motion occurs. The Eckardt frame[30] or ''molecule fixed coordinate system''[29] is used because it is impossible to decouple rotational motion completely from the vibrational motion.[21,31] The frame is constructed so that its origin is at the center of mass (CM) and it rotates in such a way that the angular momentum associated with the vibrational motion vanishes to first order in displacements. In the absence of a magnetic field, the second requirement leads to the Eckardt condition, $\Sigma_i \mathbf{a}_i \times \mathbf{r}_i' = \mathbf{0}$, where the $\mathbf{a}_i$ are equilibrium positions (which are fixed vectors), the $\mathbf{r}_i'$ are positions relative to the CM, and all vectors are in the Eckardt frame.[32] The $\mathbf{r}'_i$ are related to laboratory frame position vectors via $\mathbf{r}_i' = R\ (\chi)\mathbf{R}_i$ where $\mathbf{R}_i$ is a laboratory position vector relative to the CM and $R\ (\chi)$ is an anticlockwise rotation of the axes about the normal to the plane of the dot, through an angle χ. [The notation R is used here to distinguish a rotation of axes from a rotation, R, of a vector: $R\ (\chi) = R(-\chi)$.] The Euler angle, χ, is determined from the Eckardt condition by the equation

$$\sum_i \mathbf{a}_i \times \overline{R\ (\chi)}\mathbf{R}_i = \mathbf{0}. \tag{10}$$

In the presence of a magnetic field the Eckardt condition is the same as at zero field. It can be shown (Appendix A) that this minimizes the coupling between rotational and vibrational motion in the same way as at zero field.

The Hamiltonian for electrons in a parabolic quantum dot separates[5,33] into terms describing CM and relative motion (RM), that is, $H = H_{\mathrm{CM}} + H_{\mathrm{RM}}$. The rotational-vibrational motion is described by H_{RM} which depends on $2N-2$ coordinates. One of these is associated with rotational motion and the remaining $2N-3$ with vibrational motion. The vibrational degrees of freedom are displacements, $\boldsymbol{\rho}_i$, expressed in the Eckardt frame, so that $\mathbf{r}'_i = \mathbf{a}_i + \boldsymbol{\rho}_i$, and the rotational degree of freedom is the Euler angle, χ. What is needed here is the RM Hamiltonian expressed in terms of displacements. It is convenient to anticipate that it will be used to study vibrational motion and write it in terms of normal coordinates at the outset. Thus the displacement vectors have the general form $\boldsymbol{\rho}_i = \Sigma_{j=1}^{2N-3} \mathbf{Q}_{ij} Q_j$ where the Q_j are normal coordinates and the $\mathbf{Q}_{ij}$ are elements of a transformation matrix. The derivation of the normal coordinate Hamiltonian for zero magnetic field is treated in standard texts[29,34] and the treatment is easily generalized to the case when a perpendicular magnetic field is present (Appendix A). Thus the classical RM Hamiltonian is

$$H_{\mathrm{RM}} = \frac{1}{2}\mu(L_{\mathrm{RM}} - L_v)^2 + \frac{1}{2m^*}\sum_{k=1}^{2N-3} P_k^2 + V + \frac{\omega_c}{2}L_{\mathrm{RM}}, \tag{11}$$

where the notation is similar to that used by Wilson, Decius, and Cross:[34] L_{RM} is the RM angular momentum, $L_v = \Sigma_k \mathscr{Z}_k P_k$, $\mathscr{Z}_k = \Sigma_{ij}(\mathbf{Q}_{ij} \times \mathbf{Q}_{ik}) \cdot \hat{\mathbf{k}} Q_j$, and $\mu = I_0/(I_0 + m^* \Sigma_{ij} \mathbf{a}_i \cdot \mathbf{Q}_{ij} Q_j)^2$. Here P_j is the momentum conjugate to Q_j, I_0 is the equilibrium moment of inertia, and V is the total potential (including confinement and interaction terms together with a term quadratic in the magnetic vector potential). The quantity L_v is an angular momentum associated with vibrational motion and it involves products of coordinates and momenta. Physically, the coupling of these quantities occurs because Coriolis forces appear in the moving Eckardt frame. The Hamiltonian is independent of χ which is consistent with conservation of the RM angular momentum. Although the Hamiltonian is intended for the study of vibrational excitations it is at this stage *exact* because no approximations have been made to the potential.

B. Equilibrium positions and normal modes

The equilibrium positions are found by setting the linear momenta in Eq. (11) to zero and minimizing the resulting effective potential. The condition that the minimum occurs when all the displacements are zero leads to the equations

$$\frac{m^* L_{\mathrm{RM}}^2}{I_0^2}\mathbf{a}_i - \boldsymbol{\nabla}_i V\big|_{\mathbf{r}_i'=\mathbf{a}_i} = \mathbf{0}. \tag{12}$$

These equations give all the symmetrically equivalent configurations, predict the ring shapes discussed in Sec. III and lead directly to Eq. (8). They are similar to the equations that define Lagrangian orbits in celestial mechanics.[27]

The normal modes are found in the usual way by diagonalizing the matrix of second derivatives of the potential. In the present case there is a centrifugal term as well as the potential V. Thus the effective potential is $V' \equiv \mu L_{\mathrm{RM}}^2/2 + V$ and the elements of the second derivative matrix have the general form

$$V'_{\xi_i \xi_j} = \frac{3m^{*2} L_{\mathrm{RM}}^2}{I_0^3} a_{\xi_i} a_{\xi_j} + \frac{\partial^2 V}{\partial \xi_i \partial \xi_j}, \tag{13}$$

where the ξ_i denote components of $\mathbf{r}_i'$. Diagonalization of this matrix gives two CM modes, one rotational mode, and $2N-3$ vibrational modes and the latter are used to evaluate the RM Hamiltonian [Eq. (11)]. Coriolis effects have not been taken into account at this stage so the normal mode frequencies do not correspond to those of the vibrational modes.

C. Vibrational modes

The vibrational Hamiltonian, H', is found by expanding the RM Hamiltonian about one of the symmetrically equivalent equilibrium configurations. Retaining terms of second order or lower in momenta and coordinates leads to

$$H' = \frac{1}{2m^*}\sum_{j=1}^{2N-3} P_j^2 + \sum_{j=1}^{2N-3}\sum_{k=1}^{2N-3} C_{jk} Q_j P_k + \frac{m^*}{2}\sum_{j=1}^{2N-3} \omega_{nj}^2 Q_j^2, \tag{14}$$

where $C_{jk} \equiv (-L_{\mathrm{RM}}/I_0)\Sigma_i \mathbf{Q}_{ij} \times \mathbf{Q}_{ik} \cdot \hat{\mathbf{k}}$ is a Coriolis coupling coefficient and ω_{nj} is the frequency of the jth normal mode. Equation (14) gives the zeroth-order term in a systematic expansion of the Hamiltonian in powers of $1/a$ and at large angular momentum the corrections to H' are of order $1/\sqrt{|L_{\mathrm{RM}}|}$. This can be shown by arranging the Taylor expansions of μ and V in powers of $1/I_0$ and using the approximation $|L_{\mathrm{RM}}| \simeq \Omega I_0$ which follows from Eq. (9).

The vibrational modes are determined by assuming harmonic time dependence and using the Hamiltonian equations of motion. This leads to the following eigenvalue problem for the vibrational frequencies, ω,

$$\begin{pmatrix} V & C \\ C^T & T \end{pmatrix}\begin{pmatrix} \mathbf{q} \\ \mathbf{p} \end{pmatrix} = i\omega \begin{pmatrix} -\mathbf{p} \\ \mathbf{q} \end{pmatrix}, \tag{15}$$

where $T_{jk} = (1/m^*)\delta_{jk}$, $V_{jk} = m^* \omega_{nj}^2 \delta_{jk}$, C is the matrix of Coriolis coupling coefficients, and $\mathbf{q}$ and $\mathbf{p}$ are vectors of amplitudes. It is convenient to write this equation in the form $W\mathbf{x} = i\omega M^{-1}\mathbf{x}$ where,

$$W = \begin{pmatrix} V & C \\ C^T & T \end{pmatrix}, \quad M = \begin{pmatrix} 0 & E \\ -E & 0 \end{pmatrix}, \tag{16}$$

$\mathbf{x}^T = (\mathbf{q}^T, \mathbf{p}^T)$ and E is the unit matrix. This type of eigenvalue problem is often encountered in classical mechanics, for example, in discussions of orbital stability, and its properties are well understood. The modes come in pairs with frequencies $\pm\omega$ and they are orthogonal, in the sense that if $\mathbf{q}_j^{\pm}$ and $\mathbf{p}_j^{\pm}$ are positive and negative frequency eigenvector components then $\mathbf{p}_j^- \cdot \mathbf{q}_k^+ - \mathbf{q}_j^- \cdot \mathbf{p}_k^+ = 0$ unless $j=k$. If there are degenerate modes, linear combinations of them can be found such that this property holds. The eigenvectors can be normalized such that the matrix, K, whose columns are eigenvectors, satisfies the relation

$$MK^T M^{-1} K = E. \tag{17}$$

The proofs of these statements are given in standard texts on classical mechanics.[27,35] In the present work, K is defined such that the first $2N-3$ columns correspond to positive frequencies, that is,

$$K = \begin{pmatrix} \mathsf{Q}^+ & \mathsf{Q}^- \\ \mathsf{P}^+ & \mathsf{P}^- \end{pmatrix}, \tag{18}$$

where $\mathsf{Q}^{\pm}$ and $\mathsf{P}^{\pm}$ denote matrices whose columns are positive or negative frequency eigenvector components. Further, in the present work, all the frequencies, ω, are real so $\mathbf{q}^-$ and $\mathbf{p}^-$ are the complex conjugates of $\mathbf{q}^+$ and $\mathbf{p}^+$. Thus Q^- and P^- have the form

$$\mathsf{Q}^- = i\mathsf{Q}^{+*}, \quad \mathsf{P}^- = i\mathsf{P}^{+*}, \tag{19}$$

where the factors of i are required to normalize the eigenvectors according to Eq. (17) and this equation itself takes the form

$$\begin{pmatrix} -i\mathsf{Q}^{+*T}\mathsf{P}^+ + i\mathsf{P}^{+*T}\mathsf{Q}^+ & \mathsf{Q}^{+*T}\mathsf{P}^{+*} - \mathsf{P}^{+*T}\mathsf{Q}^{+*} \\ \mathsf{Q}^{+T}\mathsf{P}^+ - \mathsf{P}^{+T}\mathsf{Q}^+ & +i\mathsf{Q}^{+T}\mathsf{P}^{+*} - i\mathsf{P}^{+T}\mathsf{Q}^{+*} \end{pmatrix} = \begin{pmatrix} E & 0 \\ 0 & E \end{pmatrix}. \tag{20}$$

V. QUANTUM ROTATIONAL-VIBRATIONAL STATES

A. Quantum Hamiltonian

The quantum RM Hamiltonian can be derived the same way as the classical one; however, the noncommutativity of quantum coordinates and momenta leads to the presence of an extra term called the Watson term.[29,37,38] This has the form $-\hbar^2\mu/8$ but it is of order $1/L_{\mathrm{RM}}$ so does not contribute

to the vibrational Hamiltonian to the order considered here. Thus the quantum RM Hamiltonian has the same form as the classical one [Eq. (11)]. It depends on the angular momentum operator $-i\hbar\partial/\partial\chi$ but does not depend on χ. Therefore the RM wave function has the exact factorization $\psi_{\mathrm{RM}}=\exp(-iJ_{\mathrm{RM}}\chi)f_{\mathrm{RM}}$, where f_{RM} is a function of $2N-3$ normal coordinates. Making this separation and performing a harmonic expansion leads to the quantum vibrational Hamiltonian which is given by Eq. (14) with the classical variables replaced by operators.

B. Quantum vibrational states

To find the quantum vibrational states it is necessary to diagonalize the Hamiltonian defined by Eq. (14) in which coordinates and momenta are coupled. The classical vibrational Hamiltonian can be simplified by a canonical transformation[27,35,36] and a similar transformation can be used to diagonalize the quantum Hamiltonian, but as far as the author is aware this has not been mentioned in the literature. To diagonalize the quantum Hamiltonian new operators are defined by the relations

$$a_j^+=\frac{i}{\sqrt{\hbar}}\sum_k -\mathsf{Q}_{jk}^{-T}P_k+\mathsf{P}_{jk}^{-T}Q_k,$$

$$a_j=\frac{1}{\sqrt{\hbar}}\sum_k \mathsf{Q}_{jk}^{+T}P_k-\mathsf{P}_{jk}^{+T}Q_k.$$

These operators obey the commutation relations $[a_j^+,a_k^+]=[a_j,a_k]=0$, $[a_j,a_k^+]=\delta_{j,k}$ and when the Hamiltonian is expressed in terms of them it becomes $\Sigma_j\hbar\omega_j(a_j^+a_j+1/2)$. Thus all the states of the system can be expressed as powers of the a_j^+ operating on the ground state. The ground state itself is determined from the condition that it is annihilated by all the a_j, that is,

$$\left[\sum_{k=1}^{2N-3}\frac{\hbar}{i}\mathsf{Q}_{jk}^{+T}\frac{\partial}{\partial Q_k}-\mathsf{P}_{jk}^{+T}Q_k\right]f_{\mathrm{GS}}(Q_1,\ldots,Q_{2N-3})=0, \tag{21}$$

for all j. It is easy to verify that this requirement is satisfied when

$$f_{\mathrm{GS}}(Q_1,\ldots,Q_{2N-3})=\exp\left(\frac{i}{2\hbar}\sum_{k=1}^{2N-3}\sum_{k'=1}^{2N-3}\Lambda_{kk'}Q_kQ_{k'}\right), \tag{22}$$

where $\Lambda=(\mathsf{Q}^{+T})^{-1}\mathsf{P}^{+T}$ is a symmetric matrix. The symmetry follows from the orthogonality condition $\mathsf{P}^{+T}\mathsf{Q}^+-\mathsf{Q}^{+T}\mathsf{P}^+=0$ [Eq. (20)].

C. Symmetry properties of vibrational states

The symmetry properties of the vibrational states are needed to simplify the construction of antisymmetric states. As usual, the symmetry operators of the normal mode Hamiltonian are spatial transformations of the displacement vectors combined with permutations of the points to which the displacements are attached.[29] That is, a symmetry operation, O, transforms the displacements according to

$$\boldsymbol{\rho}_i'=O\boldsymbol{\rho}_{p^{-1}(i)}, \tag{23}$$

$$O\mathbf{a}_i=\mathbf{a}_{p(i)}, \tag{24}$$

where the second equation defines the permutation, $p(i)$. The equilibrium structures considered here have m-fold rotational symmetry and their point group is generally C_{mv}. The only spatial symmetries of the vibrational Hamiltonian are rotations because the Coriolis coupling breaks mirror symmetry. Therefore the spatial symmetry group of H' is the cyclic group, C_m. The full symmetry group of H' also contains mirror operators, σ, combined with time reversal, τ.

It is important to know how the quantum vibrational states transform under rotations. The matrix that transforms the normal modes is block diagonal and its blocks are the irreducible representation (irrep) matrices of the point group. The matrix that transforms them is

$$K^{-1}\begin{pmatrix}\mathsf{D}_Q & 0\\ 0 & \mathsf{D}_Q\end{pmatrix}K=\begin{pmatrix}-i\mathsf{Q}^{+*T}\mathsf{D}_Q\mathsf{P}^++i\mathsf{P}^{+*T}\mathsf{D}_Q\mathsf{Q}^+ & \mathsf{Q}^{+*T}\mathsf{D}_Q\mathsf{P}^{+*}-\mathsf{P}^{+*T}\mathsf{D}_Q\mathsf{Q}^{+*}\\ \mathsf{Q}^{+T}\mathsf{D}_Q\mathsf{P}^+-\mathsf{P}^{+T}\mathsf{D}_Q\mathsf{Q}^+ & +i\mathsf{Q}^{+T}\mathsf{D}_Q\mathsf{P}^{+*}-i\mathsf{P}^{+T}\mathsf{D}_Q\mathsf{Q}^{+*}\end{pmatrix}, \tag{25}$$

where $\mathsf{D}_Q\equiv\mathsf{D}_Q(R)$ is the matrix that transforms the normal modes, $R\in C_m$, and the right-hand side has been obtained with the aid of Eqs. (17–19). A symmetry operation cannot mix raising and lowering operators; otherwise it would not leave the Hamiltonian invariant. Therefore the off-diagonal blocks in Eq. (25) must vanish. The two diagonal blocks are complex conjugates of each other because $\mathsf{D}_Q(R)$ is real. Therefore, the transformation matrix for the raising and lowering operators has the general form

$$\begin{pmatrix}\mathsf{D}_a & 0\\ 0 & \mathsf{D}_a^*\end{pmatrix}. \tag{26}$$

The matrix $\mathsf{D}_a\equiv\mathsf{D}_a(R)$ is diagonal when all the vibrational modes are nondegenerate. Because all the irreps of C_m are one dimensional, degeneracy in the present case can only be due to the presence of the antiunitary operations $\tau\sigma$ in the full symmetry group of H'. Dimmock and Wheeler[39] have

shown that the presence of antiunitary operations in a group does not cause additional degeneracy when $\Sigma\chi((\tau\sigma)^2)=n_g$, where the sum is over all antiunitary elements, $\chi((\tau\sigma)^2)$ are characters in an irrep of the unitary subgroup, and n_g is the order of the unitary subgroup. In the present case $(\tau\sigma)^2$ is always the identity operator, $\chi((\tau\sigma)^2)=1$ and the number of mirror operations is m. Therefore the condition of Dimmock and Wheeler is satisfied. It follows that all the vibrational modes are nondegenerate and D_a is diagonal. Further, the vanishing of the off-diagonal blocks on the right-hand side of Eq. (25) implies that D_Q commutes with Λ. Thus the ground vibrational state is symmetric under rotations and the excited states change phase. The possible phases are given by the irreps of C_m and in the present work these irreps are labeled by an integer k_v, such that an anticlockwise rotation through $2\pi/m$ is represented by $\exp(2\pi i k_v/m)$. These simple transformation properties of the vibrational states lead to a simple solution of the antisymmetrization problem.

D. Antisymmetrization

Once the vibrational states have been found, approximate eigenstates of the electrons may be obtained in the form

$$\Psi=\hat{A}\psi_{\mathrm{CM}}\psi_{\mathrm{RM}}\psi_{\mathrm{spin}}(S_z), \tag{27}$$

$$=\hat{A}\psi_{\mathrm{CM}}\exp(-iJ_{\mathrm{RM}}\chi)\times f_{J_{\mathrm{RM}},n_1,\ldots,n_{2N-3}}(Q_1\ldots,Q_{2N-3})\psi_{\mathrm{spin}}(S_z), \tag{28}$$

where the antisymmetrization operator, $\hat{A}$, operates on laboratory frame electron coordinates, ψ_{CM} is the CM wave function (which is unaffected by antisymmetrization), f is the vibrational wave function, $n_1,\ldots,n_{2N-3}$ are the numbers of quanta in each vibrational mode, ψ_{spin} is the spin function, and S_z is the z component of the total spin, S. The antisymmetrization either gives an antisymmetric state or zero, depending on the quantum numbers $J_{\mathrm{RM}},n_1,\ldots,n_{2N-3}$, and S_z. For the quantum number combinations that lead to antisymmetric states the total energy is

$$E=E_{\mathrm{CM}}(n_{\mathrm{CM}},J_{\mathrm{CM}})+E_0+\sum_{i=1}^{2N-3}\left(n_i+\frac{1}{2}\right)\hbar\omega_i+g^*\mu_B BS_z, \tag{29}$$

where E_{CM} is the energy of the center of mass, n_{CM} and J_{CM} are the radial and angular momentum quantum numbers of the CM, and E_0 is the classical equilibrium energy given by Eqs. (7) and (8). Thus the total energy can be found very simply once the allowed combinations of quantum numbers have been identified.

The difficulty with antisymmetrizing the function in Eq. (28) is that most permutations transform the Euler angle and normal modes in a complicated way. However, the transformation properties are very simple under the subgroup of permutations that are equivalent to rotations and the physical reason for this is that these permutations cannot change one symmetrically equivalent minimum into another. To find the effect of these permutations on the Eckardt frame displacements first consider their effect on the Euler angle. In Eq. (10) the $\mathbf{a}_i$ are fixed vectors; therefore, any permutation of the $\mathbf{R}_i$ changes the Euler angle. For those permutations that are equivalent to rotations, R, in the sense of Eq. (24) the new Euler angle, χ', is easy to find because

$$\sum_i \mathbf{a}_i\times\overline{R}(\chi')\mathbf{R}_{p(i)}=\sum_i \mathbf{a}_{p^{-1}(i)}\times\overline{R}(\chi')\mathbf{R}_i$$

$$=R^{-1}\sum_i \mathbf{a}_i\times R\overline{R}(\chi')\mathbf{R}_i. \tag{30}$$

But $R\overline{R}(\chi')=\overline{R}(\chi'-\phi)$; therefore, $\chi'=\chi+\phi$ where ϕ is the angle of the rotation R. After allowing for the change in χ it is found that the Eckardt frame displacements transform according to the equation

$$\boldsymbol{\rho}_i'=R^{-1}\boldsymbol{\rho}_{p(i)}, \tag{31}$$

and on comparing this with Eq. (23) it can be seen that a permutation that is equivalent to a rotation changes the displacements by the inverse of the rotation to which it is equivalent. The effect of these permutations on ψ_{RM} is easily found because the rotational-vibrational states transform according to the irreps of C_m.

The antisymmetrization is done by a method used to find nuclear spin statistical weights of molecules.[40] Spin functions are chosen to transform like the irreps of the subgroup of rotationally equivalent permutations, C_R. This group is isomorphic to C_m and under the permutation, P_R, that is equivalent to an anticlockwise rotation through $2\pi/m$, the spin functions transform according to $P_R\psi_{\mathrm{spin}}=\exp(-2\pi i k_s/m)\psi_{\mathrm{spin}}$, where $0\leqslant k_s<m$. They can be constructed by means of projection operators—an example is given in the next section. The symmetric group can be decomposed into left cosets with respect to C_R so that $S_N=P_1C_R+\cdots+P_{n_c}C_R$, where $n_c=N!/m$ and an arbitrary permutation can be written in the form $p=P_sP_R^t$, where $P_R^t\in C_R$ and $0\leqslant t<m$. The allowed combinations of quantum numbers are found by writing $\hat{A}$ in the form $\hat{A}=(1/N!)\Sigma_{s=1}^{n_c}\Sigma_{t=0}^{m-1}(-1)^{P_s}(\pm1)^tP_sP_R^t$, where the sign depends on the parity of P_R. Substituting this into Eq. (28) leads to

$$\Psi=\sum_{t=0}^{m-1}(\pm1)^t\exp\left[\frac{-2\pi it}{m}\left(J_{\mathrm{RM}}+k_s+\sum_{i=1}^{2N-3}n_ik_v(i)\right)\right]\times(1/N!)\psi_{\mathrm{CM}}\sum_{s=1}^{n_c}(-1)^{P_s}P_s\psi_{\mathrm{RM}}\psi_{\mathrm{spin}}, \tag{32}$$

and it is clear that Ψ vanishes unless

$$J_{\mathrm{RM}}+k_s+\sum_{i=1}^{2N-3}n_ik_v(i)\equiv\begin{cases}0 \mod m, & m \text{ odd}\\ m/2 \mod m, & m \text{ even.}\end{cases} \tag{33}$$

Equation (33) is a necessary condition for the antisymmetrization to give a nonzero result and provided that the functions $P_s\psi_{\mathrm{RM}}\psi_{\mathrm{spin}}$ are independent it is also sufficient as shown by Wilson.[40] An alternative way of proving sufficiency is to use the Frobenius reciprocity theorem. If the functions $P_s\psi_{\mathrm{RM}}\psi_{\mathrm{spin}}$ are independent they form a basis for the representation (rep) of S_N induced by the irrep, Γ, of

C_R in which P_R is represented by ± 1. According to the reciprocity theorem the number of times the induced rep contains the antisymmetric irrep is equal to the number of times the rep of C_R subduced from the antisymmetric irrep of S_N contains Γ. This number is $(1/m)\Sigma_{t=0}^{m-1}(\pm 1)^t(\pm 1)^t=1$. Therefore Eq. (32) gives an antisymmetric state only when Eq. (33) is satisfied. Physically, Eq. (32) expresses Ψ as a linear combination of rotational-vibrational states localized on the n_c symmetrically equivalent minima.

The magic numbers are a direct consequence of Eq. (33). For a ground state the number of quanta in each vibrational mode is zero and $J_{\rm CM}=0$. Therefore the angular momentum and spin combinations of ground states are restricted to those that satisfy $J+k_s\equiv 0 \bmod m$ when m is odd and $J+k_s\equiv m/2 \bmod m$ when m is even. For spin-polarized states this condition is particularly simple because $\psi_{\rm spin}$ is symmetric and $k_s=0$. Then the possible angular momenta of the ground state are $J=N(N-1)/2+kN$ and $J=N(N-1)/2+k(N-1)$ where k is an integer, for N and $(N-1)$-fold symmetry, respectively. This is in exact agreement with Fig. 1, earlier results,[5,6] and a recent composite fermion approach.[41,42] A further discussion is given in Secs. VII and VIII after the accuracy of the vibrational approximation has been tested for the three-electron case.

VI. THREE INTERACTING ELECTRONS

A. Normal modes

The equilibrium configuration of three electrons is an equilateral triangle with the radius of each electron orbit given by Eq. (8). Standard methods for finding the normal modes are described in the literature,[34] including a detailed treatment of molecules with C_{3v} symmetry,[43] but in the present case it is simpler to use Jacobi coordinates to eliminate the CM motion at the outset. It has been verified that this approach gives the same results as the standard one. The Jacobi coordinates are given by the orthogonal transformation

$$\begin{pmatrix}\mathbf{u}_1\\ \mathbf{u}_2\\ \mathbf{u}_3\end{pmatrix}=\begin{pmatrix}1/\sqrt{2} & -1/\sqrt{2} & 0\\ 1/\sqrt{6} & 1/\sqrt{6} & -\sqrt{2/3}\\ 1/\sqrt{3} & 1/\sqrt{3} & 1/\sqrt{3}\end{pmatrix}\begin{pmatrix}\mathbf{r}_1\\ \mathbf{r}_2\\ \mathbf{r}_3\end{pmatrix}, \quad (34)$$

where $\mathbf{u}_3$ is the redundant CM coordinate. $\mathbf{u}_1$ and $\mathbf{u}_2$ are best expressed in polar coordinates with $\theta'=a\theta$ as the angular coordinate and a the radius given by Eq. (8). The advantage of this is that mixed derivatives such as $\partial^2 V'/\partial u_i \partial \theta_j'$ vanish and the second derivative matrix has the block diagonal form,

$$\begin{pmatrix}\mathsf{V}_{uu} & 0\\ 0 & \mathsf{V}_{\theta\theta}\end{pmatrix}. \quad (35)$$

After some tedious calculations it is found that V_{uu} and $\mathsf{V}_{\theta\theta}$ are given by

$$\mathsf{V}_{uu}=\frac{m^*}{4}\begin{pmatrix}9\Omega^2+\omega_r^2 & 3(\Omega^2+\omega_r^2)\\ 3(\Omega^2+\omega_r^2) & 9\Omega^2+\omega_r^2\end{pmatrix}, \quad (36)$$

$$\mathsf{V}_{\theta\theta}=\frac{m^*}{4}\begin{pmatrix}3\Omega^2+\omega_r^2 & -3(\Omega^2-\omega_r^2)\\ -3(\Omega^2-\omega_r^2) & 3\Omega^2+\omega_r^2\end{pmatrix},$$

where $\omega_r=|L_{\rm RM}|/I_0$. The second derivative matrix is easily diagonalized. Its eigenvectors form the columns of the matrix,

$$\frac{1}{\sqrt{2}}\begin{pmatrix}1 & 1 & 0 & 0\\ 1 & -1 & 0 & 0\\ 0 & 0 & 1 & 1\\ 0 & 0 & -1 & 1\end{pmatrix}. \quad (37)$$

The first column is a radial mode whose frequency is given by $\omega_1^2=3\Omega^2+\omega_r^2$, the next two columns are bending modes whose frequency is given by $\omega_2^2=(3\Omega^2-\omega_r^2)/2$, and the final column is a pure rotational mode of frequency ω_r. The radial mode has no angular displacements. The bending modes do have angular displacements in addition to radial displacements but the displacement pattern is not unique because the bending modes are degenerate.[34,43] The first three columns give the vibrational degrees of freedom and are used to find the vibrational mode frequencies. The corresponding normal coordinates are denoted by Q_1, Q_2, and Q_3, respectively.

It is interesting to compare the present results with those of Schweigert and Peeters,[23] who have calculated the normal modes of up to 50 parabolically confined classical interacting electrons in the absence of a magnetic field and at zero angular momentum. They find that the radial mode has frequency $\sqrt{3}\omega_0$ independent of the electron number and this is identical to the zero field and zero angular momentum limit of ω_1. At finite angular momentum and in the presence of a magnetic field it can be shown that the radial mode frequency is given by $\omega_1^2=3\Omega^2+\omega_r^2=3\Omega^2+L_{\rm RM}^2/I_0^2$ for all electron numbers. In contrast to the zero angular momentum case this has some electron number dependence because I_0 depends on N.

B. Vibrational modes

The vibrational frequencies are obtained from the solution of the eigenvalue problem defined in Eq. (15) and the definition of the Coriolis coupling coefficients given in Sec. IV C. All the Coriolis coupling coefficients except C_{23} and C_{32} vanish. Physically, this means that Coriolis coupling has no effect on the radial mode but splits the degenerate bending modes. The splitting is given by the solution of

$$\begin{vmatrix} m^*\omega_2^2 & 0 & i\omega & \omega_r\\ 0 & m^*\omega_2^2 & -\omega_r & i\omega\\ -i\omega & -\omega_r & 1/m^* & 0\\ \omega_r & -i\omega & 0 & 1/m^*\end{vmatrix}=0, \quad (38)$$

which has been obtained from Eq. (15) with the aid of the relation $C_{23}=-C_{32}=\omega_r$, where the sign of C_{23} corresponds to a negative angular momentum ($L_{\rm RM}=-\hbar J_{\rm RM}$ and $J_{\rm RM}>0$ for the cases of interest here). The solutions of Eq. (38) are $\omega_\pm^2=(\omega_2\pm\omega_r)^2$ and the corresponding eigenvectors give the matrices Q^+ and P^+:

$$\mathsf{Q}^{+}=\begin{pmatrix} -i/\sqrt{2m^{*}\omega_1} & 0 & 0 \\ 0 & -i/(2\sqrt{m^{*}\omega_2}) & -i/(2\sqrt{m^{*}\omega_2}) \\ 0 & -1/(2\sqrt{m^{*}\omega_2}) & 1/(2\sqrt{m^{*}\omega_2}) \end{pmatrix}, \tag{39}$$

$$\mathsf{P}^{+}=\begin{pmatrix} \sqrt{m^{*}\omega_1/2} & 0 & 0 \\ 0 & \sqrt{m^{*}\omega_2}/2 & \sqrt{m^{*}\omega_2}/2 \\ 0 & -i\sqrt{m^{*}\omega_2}/2 & i\sqrt{m^{*}\omega_2}/2 \end{pmatrix},$$

where the columns correspond to modes with frequencies ω_1, ω_+, and ω_-, respectively.

The importance of Coriolis coupling can be seen by comparing the frequencies of the vibrational modes with those of the normal modes. Equation (9) gives $\omega_r \simeq \Omega$; thus the Coriolis coupling terms are at least of order ω_0, which is not small. Further, in the high magnetic-field limit $\Omega \simeq \omega_c/2$. This leads to the relations $\omega_1 \simeq \omega_+ \simeq \omega_c$ and $\omega_- \simeq 0$. Thus ω_1 and ω_+ correspond to inter-Landau-level excitations and ω_- corresponds to an intra-Landau-level excitation. These are precisely the excitations one would expect on physical grounds. In contrast, the high field limit of the bending mode frequency, $\omega_2 \simeq \omega_c/2$, does not correspond to any physical excitation frequency. Thus the normal mode frequencies give a poor approximation to the excitation spectrum and it is necessary to take account of Coriolis coupling.

The symmetry properties of the vibrational states are easily obtained from Eqs. (25) and (39). After taking into account the coordinate transformations defined by Eqs. (37) and (34) it is found that the transformation matrix D_a for a $2\pi/3$ anticlockwise rotation is

$$\begin{pmatrix} 1 & 0 & 0 \\ 0 & \exp(-2\pi i/3) & 0 \\ 0 & 0 & \exp(2\pi i/3) \end{pmatrix}. \tag{40}$$

Both the diagonal form and the nondegeneracy of the vibrational modes are in accordance with the general discussion of Sec. V C. The vibrational ground state follows from Eqs. (39) and (22): $f_{\mathrm{GS}}(Q_1,Q_2,Q_3)=\exp\{-m^{*}[\omega_1 Q_1^2+\omega_2(Q_2^2+Q_3^2)]/2\hbar\}$. This happens to be the same as the normal mode ground state and is clearly symmetric under $2\pi/3$-fold rotations.

C. Antisymmetrization

The antisymmetrization is carried out according to the prescription of Sec. V D. This requires spin functions that transform according to the irreps of C_R and they can be obtained with the aid of the projection operator $(1/m)\Sigma_{t=0}^{m-1}\varepsilon^t P_R^t$, where $\varepsilon=\exp(2\pi i k_s/m)$. Except for a normalization factor this gives

$$S_z=\tfrac{3}{2}: \quad |\uparrow\uparrow\uparrow\rangle, \tag{41}$$

$$S_z=\tfrac{1}{2}: \quad |\uparrow\uparrow\downarrow\rangle+\varepsilon|\downarrow\uparrow\uparrow\rangle+\varepsilon^2|\uparrow\downarrow\uparrow\rangle, \tag{42}$$

for $S_z>0$ and there are similar functions for $S_z<0$. Because the spatial part of the Hamiltonian is independent of spin, it is only necessary to consider spin functions for one of the possible S_z values for each distinct value of S. These are chosen to be the $k_s=0$ function in Eq. (41) which leads to states with $S=3/2$ and $S_z=3/2$ and the $k_s=1$ and $k_s=2$ functions in Eq. (42) which lead to states with $S=1/2$ and $S_z=1/2$. The remaining spin functions simply give states with different Zeeman energies. What is of particular interest here are the ground-state and the low-lying excitations. At high magnetic field all the low-lying excitations are intra-Landau-level excitations which have a few quanta of $\hbar\omega_-$. Equation (40) shows that the intra-Landau-level mode has $k_v=1$; therefore, the condition for an antisymmetric state [Eq. (33)] reduces to $J_{\mathrm{RM}}+n_-+k_s\equiv 0 \bmod 3$, where n_- is the number of quanta of $\hbar\omega_-$. The allowed combinations of J_{RM}, n_-, and S are given in Table I.

TABLE I. Combinations of J_{RM}, n_-, and S satisfying the condition $J_{\mathrm{RM}}+n_-+k_s\equiv 0 \bmod 3$. The S value for each combination of J_{RM} and n_- is given.

	$J_{\mathrm{RM}}\equiv 0 \bmod 3$	$J_{\mathrm{RM}}\equiv 1 \bmod 3$	$J_{\mathrm{RM}}\equiv 2 \bmod 3$
$n_-\equiv 2 \bmod 3$	1/2	3/2	1/2
$n_-\equiv 1 \bmod 3$	1/2	1/2	3/2
$n_-\equiv 0 \bmod 3$	3/2	1/2	1/2

D. Comparison with numerical results

Before the approximate results can be compared with the results of an exact diagonalization, it is necessary to determine how the RM quantum numbers in Table I combine with the quantum numbers of the CM. When the total angular momentum is magic the ground RM state combines with the ground CM state ($J_{\mathrm{CM}}=0$) to give the overall ground state so $J=J_{\mathrm{RM}}$. At nonmagic angular momenta there are two possibilities. Either the state of lowest overall energy is a magic RM state with $J_{\mathrm{RM}}<J$ combined with an excited CM state with $J_{\mathrm{CM}}=J-J_{\mathrm{RM}}$, or it is a nonmagic RM state with $J=J_{\mathrm{RM}}$ combined with the CM ground state. In all cases the approximate ground-state energy can be written in the form

$$E_{\mathrm{GS}}=E_{\mathrm{CM}}(0,0)+E_0+E_{\mathrm{zp}}+g^{*}\mu_B B S_z+E_x, \tag{43}$$

where $E_{\mathrm{CM}}(0,0)$ is the ground-state energy of the CM and E_{zp} is the quantum zero point energy of the vibrational states. The energy E_x vanishes when J is magic. Otherwise it is either a CM excitation energy or the energy of the minimum number of vibrational quanta in the RM ground state, depending on which of these two energies is the lowest. For three electrons the CM excitations are found to occur only when $S=3/2$ and $J\equiv 1 \bmod 3$. In this case $J_{\mathrm{CM}}=1$, $J_{\mathrm{RM}}=J-1$, and Eq. (3) gives $E_x=\hbar(\Omega-\omega_c/2)$. At all other J,S combinations E_x is a multiple of $\hbar\omega_-$ as shown in Table I, for example, $E_x=\hbar\omega_-$ when $S=3/2$ and $J\equiv 2 \bmod 3$.

Ground-state energies calculated from Eq. (43) are shown in Figs. 3 and 4 (upper frames) for $S=3/2$ and $S=1/2$, respectively. Each figure shows the ground-state energy as a function of the total angular momentum, J, that is, the lowest energy for each J. The magnetic field is 20 T so the absolute ground state has a relatively large angular momentum and the vibrational approximation might be expected to work reasonably well. The diamonds give the results of an exact numerical diagonalization, the squares give the results of the

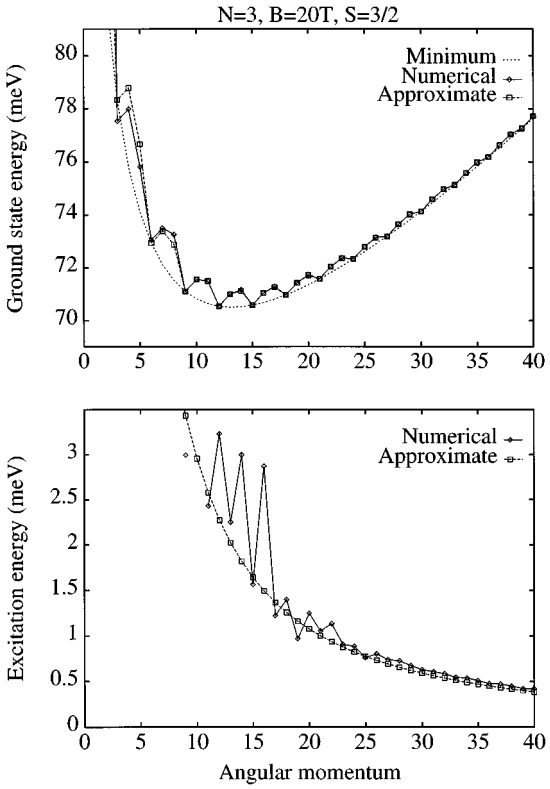

FIG. 3. Comparison of numerical and approximate ground-state energies for three interacting electrons with spin $S=3/2$ at magnetic field $B=20$ T. The upper frame shows the ground-state energy against the total angular momentum quantum number J. The lower frame gives the lowest RM excitation against the relative angular quantum number J_{RM}.

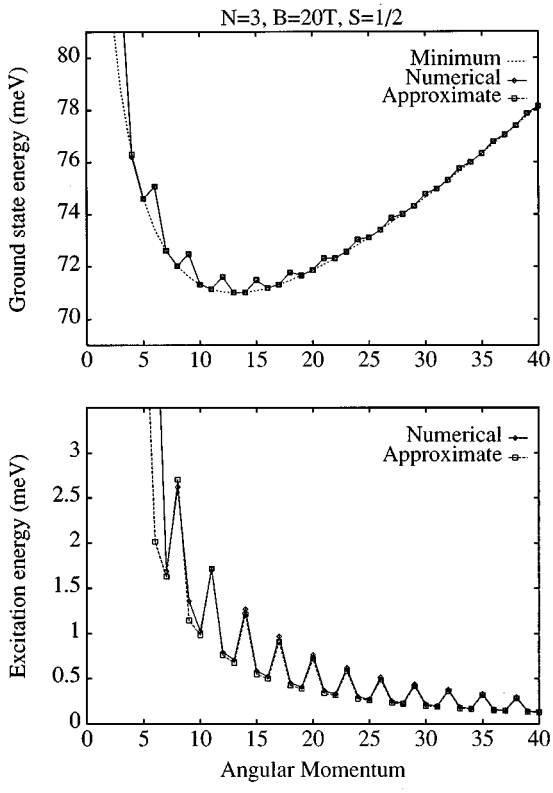

FIG. 4. Comparison of numerical and approximate ground-state energies for three interacting electrons with spin $S=1/2$ at magnetic field $B=20$ T. The upper frame shows the ground-state energy against the total angular momentum quantum number J. The lower frame gives the lowest RM excitation against the relative angular quantum number J_{RM}.

approximation, and the lines are to guide the eye. Clearly, the approximate and exact results agree very well indeed. The minima at the magic J values are well reproduced and the numerical and approximate points are almost indistinguishable throughout the J range when $S=1/2$ and for J greater than about 10 when $S=3/2$. As an example of the accuracy at large J, the numerical ground-state energy at $J=30$ and $S=3/2$ is 74.1341 ± 0.0001 meV while the approximate energy is 74.1332 ± 0.0002 meV. The uncertainty in the numerical result is due to the truncation of the basis at four Landau levels and the finite number of iterations used to find the energy eigenvalue, while the uncertainty in the approximate result is due to the finite number of the Newton-Raphson steps used to solve Eq. (8). The high accuracy at large J is probably due to the fact that all first order matrix elements of the anharmonic terms in the RM Hamiltonian vanish. Thus the higher-order corrections to the energy, which at first sight are of order $1/\sqrt{|L_{\mathrm{RM}}|}$, are actually of order $1/L_{\mathrm{RM}}$. Nevertheless, the accuracy of the approximation at low J is remarkable.

RM excitation energies are also shown in Figs. 3 and 4 (lower frames). The figures show the lowest RM excitation energy as a function of the relative angular momentum, J_{RM}. The excitation energies can be deduced from Table I. When $S=3/2$ the excitation energy is $3\hbar\omega_-$ for all values of J_{RM} but when $S=1/2$ the excitation energy is $2\hbar\omega_-$ when $J_{\mathrm{RM}}\equiv 2 \mod 3$ and $\hbar\omega_-$, otherwise. The diamonds in the figures give exact numerical results, the squares give approximate results, and the lines are to guide the eye. There are no exact results at $J_{\mathrm{RM}}=10$ and $J_{\mathrm{RM}}\leqslant 8$ because there are no intra-Landau-level excitations in these cases. The exact results are broadly in agreement with the approximate ones. When $S=1/2$ (Fig. 4) the approximation is very good and, in particular, the oscillations in the excitation energy are well reproduced. When $S=3/2$ the approximation is accurate to about 8% in the large angular momentum limit, but at low angular momenta the numerical excitation energy fluctuates although the general trend is in agreement with the approximation. The fluctuations could be caused by tunneling between symmetrically equivalent minima or by anharmonicity. They coincide with the range of J values where only two $S=3/2$ RM states can be constructed from the zeroth Landau level ψ_{nl} (except for $J=10$) and they are much less apparent in the $S=1/2$ case when the Hilbert space is larger.

The curves labeled ''minimum'' (Figs. 3 and 4) show the energy obtained by setting $E_x=0$ in Eq. (43). This gives a lower bound to the total energy and serves to illustrate the small energy scale of the magic number effects. $\hbar\omega_-\simeq 0.76$ meV when $J=12$ which is about 1% of the total energy. Further, E_{zp} depends weakly on J unless $J\simeq 0$. The only term that is both large and strongly J dependent is the classical minimum term, E_0; thus the J value of the absolute

ground state is essentially determined by classical physics together with the requirement that J be a magic number. This is consistent with the observation that the position of the density maximum is very close to the classical orbit radius (Sec. III). An approximation to the ground-state J value can be found by approximating E_0 with the aid of Eq. (9). This gives

$$E_0 \simeq \left(|L_{\rm RM}|\Omega + L_{\rm RM}\frac{\omega_c}{2} \right) + \frac{e^2 N \alpha_N}{4\pi\epsilon\epsilon_0}\sqrt{\frac{m^* I_0' \Omega}{|L_{\rm RM}|}} + O\left(\frac{1}{|L_{\rm RM}|^2} \right). \tag{44}$$

When $L_{\rm RM} = -\hbar J_{\rm RM}$ and $J_{\rm RM} \geqslant 0$ the value, J^*, of $J_{\rm RM}$ that minimizes E_0 is given by

$$J^{*3/2} = \frac{1}{2}\frac{e^2 N \alpha_N}{4\pi\epsilon\epsilon_0}\frac{\sqrt{m^* I_0' \Omega}}{\hbar^{3/2}(\Omega - \omega_c/2)}. \tag{45}$$

The optimal value of $J_{\rm RM}$ is either $[J^*]$ or $[J^*]+1$, depending on which of these values gives the lowest value of E_0, where $[J^*]$ denotes the integer part of J^*. For three electrons and the parameters used to obtain Figs. 3 and 4, Eq. (45) gives $J^* = 13.15$. The optimal value of $J_{\rm RM}$ turns out to be 13 which corresponds to $S = 1/2$. For the exact results shown in Figs. 3 and 4 the ground-state J value without the Zeeman energy is indeed 13, but the Zeeman term reduces the energy of the $S = 3/2$ state so the actual ground-state J value is 12.

The most interesting experimental consequences of the results in Figs. 3 and 4 concern the magnetic-field dependence of the ground state. As mentioned in Secs. I and III, the ground-state angular momentum increases in a steplike way with magnetic field.[5–8,10,19,24] Essentially, this is because the field compresses the wave function, leading to an increase of Coulomb energy which can be compensated by the expansion of the wave function which accompanies an increase of angular momentum. Maksym, Hallam, and Weis[24] have used exact diagonalization to give a detailed analysis of this effect and it is interesting to see how it emerges from the approximations developed here. Both the increase of Coulomb energy and the compensating effect of increasing the angular momentum are contained in the classical energy given by Eq. (44). A transition occurs when $E_0(J,B) = E_0(J+1,B)$ or approximately when $\partial E_0/\partial J = 0$. Thus the transition fields can be found by substituting integer values for J^* in Eq. (45). The right-hand side of this equation is a monotonically increasing function of B. This means that all J values should occur in sequence as the field is increased but in fact the Zeeman contribution to the total energy favors spin-polarized states and suppresses some of the J values associated with other spin polarizations. One example of this is the suppression of the $J = 13$ state mentioned in the preceding paragraph and others are given by Maksym and Chakraborty.[6] A more interesting property of the transitions emerges from the high-field limit of Eq. (45), which may be written in the form

$$B = \frac{m^*}{e}\left[\frac{1}{2\sqrt{2}}\frac{e^2 N \alpha_N}{4\pi\epsilon\epsilon_0}\frac{\sqrt{m^* I_0'}}{\hbar^{3/2}\omega_0^2} \right]^{-2/3} J^*. \tag{46}$$

Thus the transition field is linear in J and the spacing between transitions is *independent* of J. This explains the near regularity of transition fields which is found in results of exact diagonalizations[44] for large B. In the case of the three-electron system considered here the mean spacing, calculated by sampling the exact ground-state J value at 0.1 T intervals in the range 15–25 T, with the g factor set to zero, is 1.55 ± 0.05 T while the spacing predicted by Eq. (46) is 1.548 T. By generalizing Eqs. (7) and (8) to arbitrary power-law potentials it can be shown that the regular spacing only occurs for certain special potentials, particularly the combination of r^2 confinement with $1/r$ interactions. Thus measurements of the transition fields could provide an experimental probe of the potentials in real dots. Another interesting feature of the present results is the oscillation of the RM intra-Landau-level excitation energy of the $S = 1/2$ states. Experimental observation of this effect would require a probe that is sensitive to RM excitations, such as measurement of a thermodynamic property, together with a low g factor to ensure that all the J values allowed at $S = 1/2$ occurred.

VII. GENERAL FEATURES OF N-ELECTRON DOTS

A. Origin of magic numbers

The treatment of the magic numbers [Eq. (33)] is based on the approximation that tunneling between symmetrically equivalent minima is neglected. The results obtained so far suggest that this effect is indeed small when the angular momentum is large, but to assess the general applicability of Eq. (33) it is necessary to examine what happens when the angular momentum is small. For more than three electrons Eq. (33) predicts that ground states for different values of S can be degenerate in the absence of Zeeman splitting and the physical origin of this is the degeneracy of vibrational states localized on symmetrically equivalent minima. The degenerate levels are split by tunneling between symmetrically equivalent minima and the importance of this effect can be assessed quantitatively by exactly diagonalizing the Hamiltonian to compute the splitting. For example, in the case of four electrons Eq. (33) predicts that degenerate ground states occur at $S = 0$ and $S = 2$ when $J \equiv 2 \mod 4$ and at $S = 0$ and $S = 1$ when $J \equiv 0 \mod 4$. Numerical results indicate that the splitting of these levels rapidly decreases with J. It is at most 5% of the total energy and is typically much smaller. For the $S = 0$ and $S = 2$ levels the splitting is about 2.5 meV for $J = 2$ at 2 T, 0.9 meV for $J = 6$ at 5 T, and 0.13 meV for $J = 14$ at 10 T and the splittings of the $S = 0$ and $S = 1$ levels are about a factor of 2 smaller. At the highest field this is less than the Zeeman splitting. This suggests that the effect of tunneling between symmetrically equivalent minima is relatively small except at very small angular momenta and the predictions of Eq. (33) should be accurate for fields above a few Tesla. This is the field range where ''molecular'' states occur and the general conclusion that the ''molecular'' states are insensitive to tunneling is in agreement with the work of Häusler and Kramer.[17]

Another question is whether the ground states of electrons in a central confining potential and interacting via arbitrary pair potentials have the same magic numbers as the states of electrons in a parabolic dot. These systems have the same rotational and permutational symmetry as parabolic dots and

can be treated in the way described in Sec. V except that it is no longer possible to separate the CM motion. This does not affect the symmetry classification of the vibrational states or its consequences. Thus the occurrence of magic numbers is not restricted to systems with parabolic confinement and Coulomb interactions and should be a very general phenomenon.

It is interesting to compare the present approach to magic numbers with earlier results due to Maksym and Chakraborty.[6] These authors observed that when the exact Hamiltonian is diagonalized in a Slater determinant basis, certain special determinants occur in spin-polarized ground states only if their J values are magic. For $N \leqslant 5$ the special determinants have all the electrons in a compact cluster in the zeroth Landau level. That is, all the occupied single-electron orbitals have $n=0$ and are adjacent in angular momentum space. For example, in the calculations leading to Fig. 1, the determinant $|6\ 7\ 8\ 9\ 10\rangle$ occurs with a probability of 13% in the $J=40$ state of five electrons at 20 T. For $N>5$, when $(N-1)$-fold symmetry occurs, the special determinants have one electron with $l=0$ and the remaining electrons in a compact cluster, for example, $|0\ 8\ 9\ 10\ 11\ 12\rangle$ occurs with a probability of 18% in the $J=50$ state of six electrons at 17.5 T (Fig. 1). In each case the probability of the compact clusters is about a factor of 2 greater than that of the next most probable state. Maksym and Chakraborty showed that the Coulomb energy of the compact cluster states is reduced by an exchange contribution whose magnitude is exceptionally large. This leads to a reduction in the total energy and makes the magic J values favorable. It is easy to calculate the possible J values of the compact cluster states and show that they are in agreement with the expressions for the magic numbers of spin-polarized systems given in Sec. V C. Further insight into the properties of the compact cluster states can be obtained by calculating the pair-correlation function $P_{ss'}(\mathbf{r},\mathbf{r}_0)$. When the system is spin-polarized the pair-correlation function for an arbitrary Slater determinant composed of Fock-Darwin states is given by

$$P(\mathbf{r},\mathbf{r}_0)=\frac{(2\pi\lambda^2)^2}{N(N-1)}\sum_{ij}\ |\psi_{n_il_i}(\mathbf{r})|^2|\psi_{n_jl_j}(\mathbf{r}_0)|^2 - \psi_{n_il_i}(\mathbf{r})^*\psi_{n_jl_j}(\mathbf{r}_0)^*\psi_{n_il_i}(\mathbf{r}_0)\psi_{n_jl_j}(\mathbf{r}), \quad (47)$$

where the spin indices on P have been suppressed. This cumbersome expression is analyzed in Appendix B. It is shown there that it is stationary when $r=r_0$. Further, when all the ψ_{nl} have $n=0$ and large l the stationary value can be approximated by

$$P(\mathbf{r},\mathbf{r}_0)=\frac{1}{2\pi\overline{l}\ N(N-1)}\ \exp\{-2(x-\sqrt{2\overline{l}\ })^2\} \times\sum_{ij}\ \{1-\cos[(e_i-e_j)(\phi-\phi_0)]\} \times[1+O(e_i+e_j)], \quad (48)$$

where $\lambda x=r=r_0$, ϕ and ϕ_0 are polar angles, $\overline{l}$ is the average angular momentum of the cluster, and $e_i=l_i-\overline{l}$. For compact clusters of N electrons the distribution of e_i is symmetric so the terms of order (e_i+e_j) vanish. The remaining sum reduces to $N(N-1)-2\Sigma_{p=1}^{N-1}(N-p)\cos p(\phi-\phi_0)$, which has maxima when $(\phi-\phi_0)=2\pi k/N$, where k is an integer $(k\neq 0)$. The global maxima occur when $x=\sqrt{2\overline{l}\ }$. For an N-electron cluster $\overline{l}=J/N$ and because of the relation $\lambda^2=\hbar/(2m^*\Omega)$, the condition for a maximum is equivalent to $I_0\Omega=\hbar J$. Therefore the maxima of $P(\mathbf{r},\mathbf{r}_0)$ in the high angular momentum limit have N-fold symmetry and occur when both r and r_0 take the approximate orbit radius given by Eq. (9). Compact clusters of $(N-1)$ electrons can be analyzed in a similar way except that only $N-1$ of the single-electron states are taken to have large angular momenta. Then the symmetry is $(N-1)$-fold with a peak at the origin, $\overline{l}=J/(N-1)$ and the maxima again occur at the radius given by Eq. (9). Thus the pair-correlation functions of the compact cluster states have exactly the symmetry that favors a low Coulomb energy. This explains the large exchange energy that appears when the Coulomb energy is expressed as a sum of matrix elements between eigenstates of angular momentum and provides the link between the approach of Maksym and Chakraborty and the present one.

B. Systems with competing classical minima

The physical picture of a ''molecular'' ground state localized about one classical equilibrium configuration breaks down when there are competing classical minima. Then tunneling between symmetrically inequivalent minima can result in the quantum ground state being a mixture of states with different types of symmetry. These are the liquidlike states mentioned in Secs. I and III. Because the electron-electron interaction conserves angular momentum and spin, the mixing can only occur in special cases when more than one type of symmetry is allowed to occur at the same set of magic numbers. Thus the classification of the possible magic numbers and symmetry types can be used to predict whether the ground state is molecular or not.

The six-electron system is the smallest in which classical equilibrium configurations with different symmetry have similar energies.[45] It is discussed here as an example of the effects that can occur when minima compete. The two possible classical equilibrium configurations are a fivefold ring with one electron at the center and a sixfold ring. For $J=45$ and the parameters used for the calculations leading to Fig. 1, the difference between the energies of these two configurations is only about 0.57 meV, so at first sight it is unreasonable to expect that the quantum ground state is localized about either one of them. However, according to the rules developed in Sec. V C, fivefold symmetry with full spin polarization requires that $J\equiv 0 \mod 5$ and sixfold symmetry requires $J\equiv 3 \mod 6$. Both types of symmetry occur only when $J=15,45,75\ldots$. Thus the liquidlike states can only occur at this restricted set of J values and molecular states occur at other J values. This is illustrated in Fig. 5 which shows pair-correlation functions for the six-electron system. The lower left frame $(J=50)$ is the pair-correlation function for the ground state shown in Fig. 1 and serves as a reference point. All the other states are the lowest-energy states at the indicated values of J. The pair-correlation function at $J=51$ clearly corresponds to sixfold symmetry and the one at $J=40$ to fivefold symmetry. The $J=45$ case exhibits some

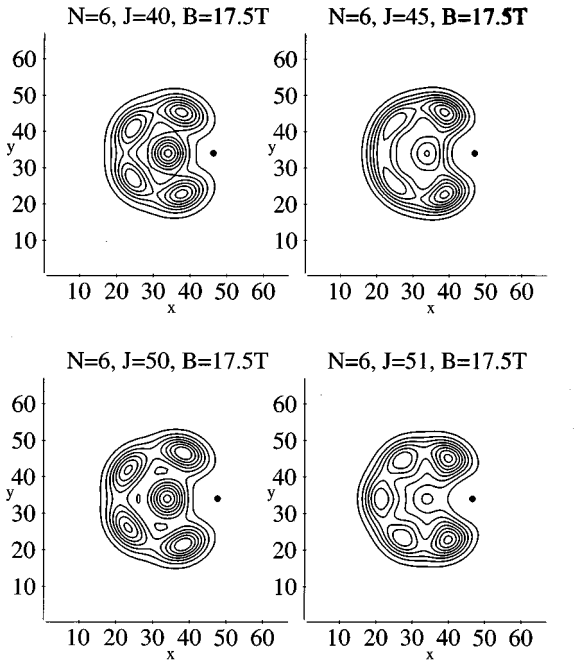

FIG. 5. Pair-correlation function $P_{ss'}(\mathbf{r},\mathbf{r}_0)$ for six interacting, spin-polarized electrons at $B=17.5$ T. Pair-correlation functions for the lowest-energy state at the indicated angular momenta are shown. The black spots denote $\mathbf{r}_0$. The x and y unit is 1.89 nm.

loss of symmetry. The peaks on the outer ring are less sharp than at $J=40$ and $J=50$ and the peak at the center is much less well defined. When these J values are converted to effective filling factors[28] with the aid of the formula, $\nu=N(N-1)/2J$, it is found that the loss of symmetry occurs only when $\nu=1/(2k+1)$, where k is a positive integer, that is, at the same odd-denominator fractions where fractional quantum Hall liquids occur. One can speculate that although the occurrence of competing minima becomes more common as the number of electrons increases, tunneling is always restricted by selection rules and conservation laws with the result that liquidlike states only occur at odd-denominator filling factors.

VIII. DISCUSSION

The Eckardt frame approach allows the quantum states of electrons in quantum dots to be understood both qualitatively and quantitatively in a comprehensive and unified way. The advantage of the approach is that the classical equilibrium configuration is stationary in the Eckardt frame. This has been used to develop a detailed treatment of molecular electron states which are localized about a single classical equilibrium configuration and can be approximated by antisymmetrized rotational-vibrational states. The approximation enables the energies of the molecular states and their low-lying excitations to be calculated accurately. In addition, the magic numbers found in previous numerical work can be derived quite simply from the requirement that the electron ground state is approximated by an antisymmetrized rotational-vibrational ground state. It is remarkable that this approach predicts exactly the same magic numbers as composite fermion theories,[41,42] and this connection with the composite fermion treatement may be a particularly fruitful area for further study. The molecular picture breaks down in the presence of quantum tunneling. Selection rules and conservation laws have been used to determine when this effect occurs and which states are affected. Tunneling between symmetrically equivalent minima simply lifts the spin degeneracy associated with certain magic angular momenta. Tunneling between symmetrically inequivalent minima has a much more important effect and, when it is allowed, leads to the formation of liquidlike states which are not localized about a single minimum. For six electrons these states only occur at odd-denominator filling factors, and whether they evolve into fractional quantum Hall liquids as the number of electrons is increased is a fascinating open question.

A possible development of the present work is to use the Eckardt frame approach as a computational tool. Tunneling between symmetrically equivalent minima could be taken into account by numerically diagonalizing the Hamiltonian in a basis of antisymmetrized states centered on the various minima. In addition, it might be possible to devise a variational approach to include the symmetrically inequivalent minima. The precision of the vibrational approximation for three electrons suggests that this might enable low-lying states of quantum dots to be calculated accurately and economically with a relatively small basis set.

We recently received results from Ruan *et al.* Using a different approach, they have related the ground-state magic numbers to the symmetry of potential minima for up to five spin-polarized electrons and obtained the same results as given here.[46]

ACKNOWLEDGMENTS

I would like to thank Dr. D. Pfannkuche for drawing my attention to the regularity of the transition fields and Dr. N. Bruce for critically reading the manuscript. This work was supported by the U.K. Engineering and Physical Sciences Research Council.

APPENDIX A: THE RM HAMILTONIAN

To find the RM Hamiltonian in the presence of a magnetic field it is sufficient to consider classical mechanics. Once the classical Hamiltonian is available, the quantum Hamiltonian can be obtained by standard methods.[34,37,38] The only issue is the form of the conjugate momenta. These can be obtained from the classical Lagrangian kinetic energy which has the form,

$$\mathscr{L}=\sum_{i=1}^{N}\frac{m^*v_i^2}{2}-e\mathbf{A}_i\cdot\mathbf{v}_i\,, \tag{A1}$$

when expressed in laboratory frame velocities, $\mathbf{v}_i$. Separating the CM terms, transforming to Eckardt frame variables as described by Wilson, Decius, and Cross[34] and expressing the vector potential in the symmetric gauge leads to

$$\mathscr{L}=\frac{I\omega'^2}{2}+m^*\boldsymbol{\omega}'\hat{\mathbf{k}}\cdot\sum_{i=1}^{N}(\boldsymbol{\rho}_i\times\boldsymbol{\rho}_i)+\sum_{i=1}^{N}\frac{m^*\dot{\rho}_i^2}{2}-\frac{I\omega_c^2}{8}, \tag{A2}$$

where I is the instantaneous moment of inertia, $\omega' = \dot{\chi} - \omega_c/2$ and the Eckardt condition has been used to eliminate $\Sigma_i(\mathbf{a}_i \times \dot{\boldsymbol{\rho}}_i)$. After expressing the displacements in terms of normal coordinates this becomes

$$\mathscr{L} = \frac{I\omega'^2}{2} + m^*\omega' \sum_{i=k}^{2N-3} \mathscr{Z}_k \dot{Q}_k + \sum_{k=1}^{2N-3} \frac{m^* \dot{Q}_k^2}{2} - \frac{I\omega_c^2}{8}, \tag{A3}$$

where $\mathscr{Z}_k = \Sigma_{ij}(\mathbf{Q}_{ij} \times \mathbf{Q}_{ik}) \cdot \hat{\mathbf{k}} Q_j$. Differentiating this to obtain the conjugate momenta yields

$$P_j = \frac{\partial \mathscr{L}}{\partial \dot{Q}_j} = m^* \dot{Q}_j + m^* \omega' \mathscr{Z}_j, \tag{A4}$$

$$L_{\mathrm{RM}} = \frac{\partial \mathscr{L}}{\partial \dot{\chi}} = \omega' I + m^* \sum_{k=1}^{2N-3} \mathscr{Z}_k \dot{Q}_k. \tag{A5}$$

The Hamiltonian kinetic energy is found by substituting these results into the expression $\dot{\chi} L_{\mathrm{RM}} + \Sigma_{k=1}^{2N-3} \dot{Q}_k P_k - \mathscr{L}$. This gives the kinetic energy terms in Eq. (11) except that μ is given by $(I - m^* \Sigma_k \mathscr{Z}_k^2)^{-1}$. The form of μ given in the text is obtained by transforming this expression in the way described by Watson.[37]

This derivation of the RM Hamiltonian is based on the same Eckardt condition that holds for zero magnetic field. It gives a Hamiltonian in which the lowest order coupling of coordinates and momenta occurs in the form $\mathscr{Z}_k P_k$, which is of second order in the displacements. Thus the zero-field Eckardt condition leads to first-order decoupling of coordinates and momenta even when a magnetic field is present. It is instructive to consider this from another point of view. Suppose an arbitrary linear transformation is used in place of the transformation to normal coordinates. Then the form of Eqs. (A2) to (A5) is unaltered but $\mathscr{Z}_k$ acquires the extra term $\Sigma_i(\mathbf{a}_i \times \mathbf{Q}_{ik}) \cdot \hat{\mathbf{k}}$. Consequently, the Hamiltonian acquires a term that is linear in P_k. However, when normal coordinates are used $\Sigma_i(\mathbf{a}_i \times \mathbf{Q}_{ik}) \cdot \hat{\mathbf{k}}$ vanishes. This follows from the orthogonality of the transformation to normal coordinates and is equivalent to the Eckardt condition. Therefore, the terms linear in P_k vanish when normal coordinates are used and, as at zero field,[21] use of normal coordinates necessarily implies use of the Eckardt frame.

APPENDIX B: THE PAIR-CORRELATION FUNCTION FOR A SLATER DETERMINANT OF FOCK-DARWIN STATES

The Fock-Darwin states [Eq. (2)] have the general form

$$\psi_{nl} = (2\pi\lambda^2)^{-1/2} \exp(-x^2/4) h_{nl}(x) \exp(-il\phi), \tag{B1}$$

where $x = r/\lambda$ and h_{nl} is real. Therefore the pair-correlation function [Eq. (47)] has the general form

$$\begin{aligned} P(\mathbf{r},\mathbf{r}_0) = \frac{1}{N(N-1)} \exp[-(x^2+x_0^2)/2] \sum_{ij} & h_{n_i l_i}^2(x) h_{n_j l_j}^2(x_0) \\ & - h_{n_i l_i}(x) h_{n_j l_j}(x_0) h_{n_i l_i}(x_0) h_{n_j l_j}(x) \\ & \times \cos[(l_i - l_j)(\phi - \phi_0)], \end{aligned} \tag{B2}$$

so the x and x_0 dependence of P has the form $\exp[-(x^2+x_0^2)/2] g(x,x_0)$. This is stationary with respect to variations in x and x_0 when $xg = \partial g/\partial x$ and $x_0 g = \partial g/\partial x_0$. By considering the derivatives of h_{nl} it can be shown that $x\partial g/\partial x = F(x,x_0)$ and $x_0 \partial g/\partial x_0 = F(x_0,x)$, where the first equation defines F. It follows from these relations that P is stationary when $x^2 = x_0^2 = F(x,x)/g(x,x)$, that is, when $x = x_0$.

It is more difficult to analyze the ϕ dependence of P. However, when $n=0$ the Fock-Darwin states have a single maximum at $x = \sqrt{2l}$. This enables $P(\mathbf{r},\mathbf{r}_0)$ to be simplified in the case when all the states have large l. By expanding the logarithm of the radial part of ψ_{0l} about $x = \sqrt{2l}$ and applying Stirling's approximation to the normalization factor, the Fock-Darwin states are approximated by

$$\psi_{0l}(\mathbf{r}) \simeq \frac{1}{\sqrt{2\pi\lambda^2}} \frac{1}{(2\pi l)^{1/4}} \exp\{-(x-\sqrt{2l})^2/2\} \exp(-il\phi). \tag{B3}$$

Substituting this into Eq. (B2) and putting $x = x_0$ leads to

$$P(\mathbf{r},\mathbf{r}_0) \simeq \frac{1}{2\pi N(N-1)} \sum_{ij} \frac{1}{\sqrt{l_i l_j}} \exp\{-(x-\sqrt{2l_i})^2 - (x-\sqrt{2l_j})^2\} \{1 - \cos[(l_i - l_j)(\phi - \phi_0)]\}. \tag{B4}$$

Finally, putting $l_i = \overline{l} + e_i$ and expanding to first order in e_i leads to Eq. (49) of Sec. VII A.

[1] R.C. Ashoori, H.L. Störmer, J.S. Weiner, L.N. Pfeiffer, K.W. Baldwin, and K.W. West, Phys. Rev. Lett. **71**, 613 (1993).

[2] B. Meurer, D. Heitmann, and K. Ploog, Phys. Rev. Lett. **68**, 1371 (1992).

[3] P.L. McEuen, E.B. Foxman, U. Meirav, M.A. Kastner, Yigdal Meir, Ned D. Wingreen, and S.J. Wind, Phys. Rev. Lett. **66**, 1296 (1991).

[4] J. Weis, R.J. Haug, K. v. Klitzing, and K. Ploog, Phys. Rev. Lett. **71**, 4022 (1993).

[5] P.A. Maksym and T. Chakraborty, Phys. Rev. Lett. **65**, 108 (1990).

[6] P.A. Maksym and T. Chakraborty, Phys. Rev. B **45**, 1947 (1992).

[7] M. Wagner, U. Merkt, and A.V. Chaplik, Phys. Rev. B **45**, 1951 (1992).

[8] P. Hawrylak and D. Pfannkuche, Phys. Rev. Lett. **70**, 485 (1993).

[9] N.F. Johnson and M.C. Payne, Phys. Rev. Lett. **70**, 1513 (1993).

[10] D. Pfannkuche and S. Ulloa, Phys. Rev. Lett. **74**, 1194 (1995).

[11] V. Halonen, P. Pietiläinen, and T. Chakraborty, Europhys. Lett. **33**, 377 (1996).
[12] D. Pfannkuche and R.R. Gerhardts, Phys. Rev. B **44**, 13 132 (1991).
[13] P. Hawrylak, Phys. Rev. Lett. **71**, 3347 (1993).
[14] S.R. Yang, A.H. MacDonald, and M.D. Johnson, Phys. Rev. Lett. **71**, 3194 (1993).
[15] J.J. Palacios, L. Martín-Moreno, G. Chiappe, E. Louis, and C. Tejedor, Phys. Rev. B **50**, 5760 (1994).
[16] W. Häusler, B. Kramer, and J. Măsek, Z. Phys. B **85**, 435 (1991).
[17] W. Häusler and B. Kramer, Phys. Rev. B **47**, 16 353 (1993).
[18] K. Jauregui, W. Häusler, and B. Kramer, Europhys. Lett. **24**, 581 (1993).
[19] P.A. Maksym, Physica B **184**, 385 (1993).
[20] P.A. Maksym, Europhys. Lett. **31**, 405 (1995).
[21] C. Eckardt, Phys. Rev. **47**, 552 (1935).
[22] V.M. Bedanov and F.M. Peeters, Phys. Rev. B **49**, 2667 (1994).
[23] V.A. Schweigert and F.M. Peeters, Phys. Rev. B **51**, 7700 (1995).
[24] P.A. Maksym, L.D. Hallam, and J. Weis, Physica B **212**, 213 (1995).
[25] L.D. Hallam, J. Weis, and P.A. Maksym, Phys. Rev. B **53**, 1452 (1996).
[26] D. Pfannkuche, V.A. Gudmundsson, and P.A. Maksym, Phys. Rev. B **47**, 2249 (1992).
[27] C.L. Siegel and J.K. Moser, *Lectures on Celestial Mechanics* (Springer, Berlin, 1971).
[28] S.M. Girvin and T. Jacah, Phys. Rev. B **28**, 4506 (1984).
[29] P.R. Bunker, *Molecular Symmetry and Spectroscopy* (Academic, New York, 1979).
[30] J.D. Louck and H.W. Galbraith, Rev. Mod. Phys. **48**, 69 (1976).
[31] A. Sayvetz, J. Chem. Phys. **6**, 383 (1939).
[32] When particles have different masses, m_i, the Eckardt condition is $\Sigma_i m_i \mathbf{a_i} \times \mathbf{r_i'} = \mathbf{0}$.
[33] L. Brey, N.F. Johnson, and B.I. Halperin, Phys. Rev. B **46**, 10 647 (1989).
[34] E.B. Wilson, Jr., J.C. Decius, and P.C. Cross, *Molecular Vibrations* (McGraw-Hill, New York, 1955).
[35] E.T. Whittaker, *Analytical Dynamics* (Cambridge University Press, Cambridge, 1952).
[36] H. Goldstein, *Classical Mechanics* (Addison-Wesley, Reading, 1980).
[37] J.K.G. Watson, Mol. Phys. **15**, 479 (1968).
[38] J.D. Louck, J. Mol. Spectrosc. **61**, 107 (1976).
[39] J.O. Dimmock and R.G. Wheeler, in *Mathematics of Physics and Chemistry*, edited by H. Margenau and G.M. Murphy (Van Nostrand, Princeton, 1964).
[40] E.B. Wilson, Jr., J. Chem. Phys. **3**, 276 (1935).
[41] J.K. Jain and T. Kawamura, Europhys. Lett. **29**, 321 (1995).
[42] C.W.J. Beenakker and B. Rejai, Physica B **189**, 147 (1993).
[43] J.W. Leech and D. J. Newman, *How to Use Groups* (Methuen, London, 1969).
[44] Nearly regular transitions are shown in Fig. 2 of Pfannkuche and Ulloa (Ref. 10) for $B<10$ T but the regularity is more pronounced for $B>10$ T.
[45] F. Bolton and U. Rössler, Superlatt. Microstruct. **13**, 139 (1993).
[46] W.Y. Ruan, Y.Y. Liu, C.G. Bao, and Z.O. Zhang, Phys. Rev. B **51**, 7942 (1995).